



## An anthropomorphic controlled hand prosthesis system<sup>\*</sup>

Hai HUANG<sup>†1</sup>, Hong LIU<sup>2</sup>, Nan LI<sup>2</sup>, Li JIANG<sup>2</sup>, Da-peng YANG<sup>2</sup>,

Lei WAN<sup>1</sup>, Yong-jie PANG<sup>1</sup>, Gerd HIRZINGER<sup>3</sup>

<sup>(1)</sup>National Key Laboratory of Science and Technology on Autonomous Underwater Vehicle,  
 Harbin Engineering University, Harbin 150001, China)

<sup>(2)</sup>State Key Laboratory of Robot and Systems, Harbin Institute of Technology, Harbin 150001, China)

<sup>(3)</sup>Institute of Robotics and Mechatronics, German Aerospace Center, DLR, Wessling 82230, Germany)

<sup>†</sup>E-mail: haihus@163.com

Received Sept. 1, 2011; Revision accepted July 17, 2012; Crosschecked Sept. 11, 2012

**Abstract:** Based on HIT/DLR (Harbin Institute of Technology/Deutsches Zentrum für Luft- und Raumfahrt) Prosthetic Hand II, an anthropomorphic controller is developed to help the amputees use and perceive the prosthetic hands more like people with normal physiological hands. The core of the anthropomorphic controller is a hierarchical control system. It is composed of a top controller and a low level controller. The top controller has been designed both to interpret the amputee's intentions through electromyography (EMG) signals recognition and to provide the subject-prosthesis interface control with electro-cutaneous sensory feedback (ESF), while the low level controller is responsible for grasp stability. The control strategies include the EMG control strategy, EMG and ESF closed loop control strategy, and voice control strategy. Through EMG signal recognition, 10 types of hand postures are recognized based on support vector machine (SVM). An anthropomorphic closed loop system is constructed to include the customer, sensory feedback system, EMG control system, and the prosthetic hand, so as to help the amputee perform a more successful EMG grasp. Experimental results suggest that the anthropomorphic controller can be used for multi-posture recognition, and that grasp with ESF is a cognitive dual process with visual and sensory feedback. This process while outperforming the visual feedback process provides the concept of grasp force magnitude during manipulation of objects.

**Key words:** Anthropomorphic controller, Prosthetic hand, EMG recognition, Electro-cutaneous sensory feedback  
**doi:**10.1631/jzus.C1100257      **Document code:** A      **CLC number:** TP241

### 1 Introduction

Symbolizing a benchmark for robotic designers (Bicchi, 2000), human hand has currently attracted significant efforts to replicate its complicated characteristics. Impressive results of highly integrated hands have been made (Dario *et al.*, 2002), such as Utah/MIT Hand, NASA Hand, DLR Hand, HIT/DLR Hand, GiFu Hand, and Stanford/JPL Hand (Loucks *et al.*, 1987; Jacobsen *et al.*, 2001; Diftler *et al.*, 2003;

Edsinger-Gonzales, 2004; Kawasaki *et al.*, 2004; Liu H *et al.*, 2007; Wimböck *et al.*, 2007).

Recently, simple structured and lightweight anthropomorphic hands have been developed as prosthetic hands (Zollo *et al.*, 2007). For example, Otto Bock Hand and i-limb hand are used mainly as commercial prosthetic hands; UB Hand, TBM Hand, Italian Cyber Hand, and RTR Hand II are research devices (Dechev *et al.*, 2001; Lotti *et al.*, 2005; Zollo *et al.*, 2006; 2007).

By placing electrodes on the patient's forearm skin, patient's muscles activation potentials are gathered through surface electromyography (EMG) (Castellini and van der Smagt, 2009; Micera *et al.*, 2010). There are many previous classifiers which exhibit good performance on EMG classification,

<sup>\*</sup> Project supported by the National Natural Science Foundation of China (Nos. 51175106, 51209050, and 51205080), the Fundamental Research Funds for the Central Universities, China (No. HEUCFZ 1203), and the State Key Laboratory of Ocean Engineering (Shanghai Jiao Tong University) (No. 1102)  
 © Zhejiang University and Springer-Verlag Berlin Heidelberg 2012

such as Bayes (Lee and Saridis, 1984), nonlinear discriminative analysis (Graupe *et al.*, 1982), fuzzy systems (Ajiboye and Weir, 2005), and artificial neural networks (Huang and Chen, 1999). However, some problems remain to be addressed. First, the generalization ability of a classifier dominated online EMG classification accuracy and control reliability because the number of available EMG patterns for classifier training was not large enough. Second, trained by minimizing the empirical risk, some of these classifiers did not minimize their generalization errors bound for unseen EMG patterns (Liu YH *et al.*, 2007). However, in general there existed a mixed distribution between classes due to a large variation in EMG pattern distribution. As an effective method for wide range classification (Castellini and van der Smagt, 2009), the learning strategy of support vector machine (SVM) is based on the principle of structural risk minimization. In other words, it minimizes both the empirical risk (training errors) and the generalization error bound during the training (Lee *et al.*, 2010).

There is no tactile or proprioceptive feedback for subject grasping tasks. Although the EMG control system can obtain very good results, it also requires a high level of concentration, involving the risk of early muscle fatigue (Micera *et al.*, 2010). To obtain more interactive automatic control and modify the prosthesis performance, the concept of shared control has been introduced between the information extracted from EMG signals and the prosthetic controller (Kumar *et al.*, 2010). Electro-cutaneous stimulus has been widely used in many prosthesis areas such as vestibular prosthesis (Della Santina *et al.*, 2007; Davidovics *et al.*, 2011), neural stimulation (Grill and Mortimer, 1996; Merrill *et al.*, 2005), and bionic limb (Kuiken *et al.*, 2007; Rosen *et al.*, 2009). It can transform stimulus strength into grasp force magnitude, so that the patient perceives it as if coming from the amputated limb (Clement *et al.*, 2011). Electro-cutaneous stimulus has some similar characters to the vibrotactile feedback sensory system (Pylatiuk *et al.*, 2004; Antfolk *et al.*, 2010). Grasp with either of them involves dual feedback of sense and vision, thus mostly better than visual feedback only (Stepp and Matsuoka, 2011). However, subjects can more precisely and easily obtain different grasp force grades particularly when they are in sporting states.

In this paper, the anthropomorphic controller is used to realize two schemes: (1) Realize EMG multi-posture recognition by identifying 10 different motion patterns; (2) Obtain the user-prosthesis interactive control through an electro-cutaneous sensory feedback system, EMG signal recognition, and the prosthetic hand during objects grasp. The hand can also be voice controlled through the Bluetooth protocol, and thus the control system of the hand can be biologically inspired at different levels.

## 2 HIT/DLR Prosthetic Hand II and its controller scheme

HIT/DLR Prosthetic Hand II is actuated by three motors (Fig. 1). The thumb and the index finger are actuated by two different motors. The remaining three fingers are similarly designed and actuated by one motor. Each finger is equipped with a position sensor, whereas each active finger with a torque sensor at the base joint. The details of its mechanisms and the palm hardware system were discussed in Huang *et al.* (2006).



Fig. 1 HIT/DLR Prosthetic Hand II

Considering human feelings, muscles, and voice together, the hierarchical controller of HIT/DLR Prosthetic Hand II is designed to help the amputee perceive and employ the prosthetic hand more like a person with his/her physiological hand (Fig. 2). The top controller has been designed to interpret the subject's intentions gathered from the user-prosthesis interface, whereas the low level one is responsible for grasp stability. Both levels are dependent on a sensory system comprising five positions and three torque sensors, corresponding to each finger and motor. The top controller includes the ESF system, the EMG controller, and the voice controller. The signals from electrodes are transmitted to the EMG processor. They are amplified, filtered, voltage separated, and finally transformed into multi-channelled, averaged

sampling points which are as efficient as training characters.

Located in the palm, the low level controller is responsible for hand movement, position and torque sensors feedbacks. The motors are controlled through the algorithm proposed by Huang *et al.* (2010) including force and position control.

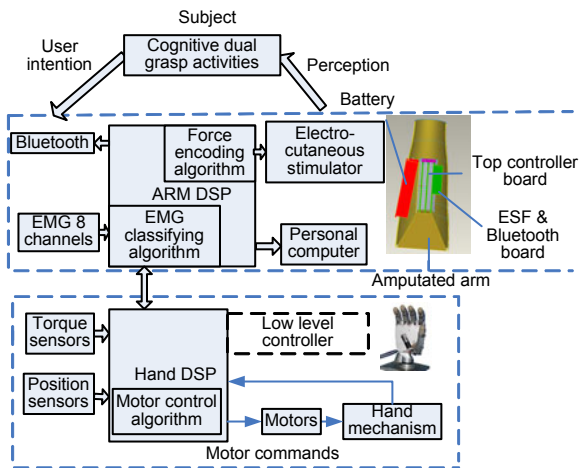


Fig. 2 Hierarchical controller system of the hand

### 3 Anthropomorphic controller system

#### 3.1 EMG control system

HIT/DLR Prosthetic Hand can perform continuous motion control (flexion/extension of selective finger motions) and realize some object grasp attitudes such as hooking, pinching, and picking with two EMG electrodes (Shimizu *et al.*, 1997; Zhao *et al.*, 2005; 2006). This study is intended to identify some more necessary motion patterns based on HIT/DLR Prosthetic Hand II mechanics, rather than decoding all the possible movement of the human hand. If we assign each of these active fingers with one degree of freedom (DOF), its relaxation, extension, and flexion are denoted as the states of 0, -1, and 1, respectively (Fig. 3). Therefore, 27 motion patterns are obtained. Among them, the basic motion patterns are illustrated in the first column; the shadowed ones are unusual in use and much more difficult to identify. Among the 19 unshadowed ones, seven basic motion patterns (1, 2, 7, 10, 15, 26, 27) and three extended ones (9, 19, 24) are more basic and useful according to human daily life and hand investigation (Taylor and Schwarz, 1955; Castellini and van der Smagt, 2009).



Fig. 3 Motion patterns of the human hand

Relaxation, extension, and flexion are denoted as 0, -1, and 1, respectively

SVM separates two data sets by placing a hyperplane so that the distance is the largest (Burges, 1998; Bitzer and van der Smagt, 2006). By introducing the slack variable  $\zeta_i$ , the following optimal support hyperplane can be obtained:

$$\begin{cases} \mathbf{w}^T \cdot \phi(\mathbf{x}_i) + b \geq 1 - \zeta_i, & \text{if } y_i = 1, \\ \mathbf{w}^T \cdot \phi(\mathbf{x}_i) + b \geq 1 + \zeta_i, & \text{if } y_i = -1, \end{cases} \quad (1)$$

$$\Leftrightarrow y_i(\mathbf{w}^T \cdot \phi(\mathbf{x}_i) + b) - 1 + \zeta_i \geq 0, \quad i = 1, 2, \dots, n,$$

where  $\mathbf{w}$  and  $b$  are the weight and bias of the hyperplane respectively,  $\zeta_i$  is the slack variable representing the error measures of data points for the nonseparable case,  $\mathbf{x}_i \in \mathbb{R}^n$  is EMG input signal corresponding to hand motion pattern, and  $\phi(\mathbf{x}_i)$  is a nonlinear mapping function which maps the data into a higher dimensional feature space from the original input space. Through  $\phi(\mathbf{x}_i)$ , the training vectors  $\mathbf{x}_i$  are mapped into a higher dimensional space where SVM finds a linear separate hyperplane with the maximal margin. If  $y_i \in \{-1, 1\}$ , we set the training samples as the pairs  $\{(x_i, y_i) | i=1, 2, \dots, n\}$  to predict whether a test sample belongs to either of the two classes.

To map the input features into a higher-dimensional dot product feature space, the radial basis function (RBF) is used (Keerthi and Lin, 2003):

$$K(\mathbf{x}_i, \mathbf{x}_j) = \exp(-\gamma \|\mathbf{x}_i - \mathbf{x}_j\|^2), \quad (2)$$

where  $\gamma$  is the kernel parameter. By introducing the following Lagrangian function, the objective of SVM for the nonlinearly nonseparable case can be solved with its dual form:

$$L(\mathbf{w}, b, \xi_i; \alpha, \beta) = \frac{1}{2} \mathbf{w}^T \mathbf{w} + C \sum_{i=1}^n \xi_i - \sum_{i=1}^n \alpha_i \xi_i - \sum_{i=1}^n \beta_i [y_i (\mathbf{w}^T \phi(\mathbf{x}_i) + b) + \xi_i - 1], \quad (3)$$

where  $C > 0$  is the regularization constant which is to be chosen by the user to balance experience risk and complication, and  $\alpha_i$  and  $\beta_i$  ( $0 \leq \beta_i, \alpha_i \leq C$ ) are non-zero Lagrange multiplier vectors, corresponding to  $\mathbf{x}_i$  which is the supporting vector of the pattern. Therefore, the dual problem can be found by differentiating the Lagrange function (4) with respect to  $\mathbf{w}$  and  $b$ :

$$\begin{aligned} \max \sum_{j=1}^n \sum_{i=1}^n \left( \beta_i - \frac{1}{2} \beta_i \beta_j y_i y_j \phi(\mathbf{x}_i) \cdot \phi(\mathbf{x}_j) \right) \\ \text{s.t. } \sum_{i=1}^n y_i \beta_i = 0, \quad 0 \leq \beta_i \leq C, \quad i = 1, 2, \dots, n. \end{aligned} \quad (4)$$

The decision function of the classification problem is

$$f(\mathbf{x}) = \text{sgn} \left( \sum_{i=1}^n \beta_i^* y_i K(\mathbf{x}_i, \mathbf{x}) + b^* \right), \quad (5)$$

where  $b^*$  is the classification threshold, and  $b^* = y_j - \sum_{i=1}^n \beta_i^* y_i K(\mathbf{x}_i, \mathbf{x}_j)$ ,  $\mathbf{w}^* = \sum_{i=1}^n \beta_i^* y_i \mathbf{x}_i$ ,  $\boldsymbol{\beta}^* = (\beta_1^*, \beta_2^*, \dots, \beta_n^*)^T$  is the solution to dual problem (5),  $j \in \{j | 0 \leq \beta_j^* \leq C\}$ .

For multi-class motion pattern recognition of the hand, the one-against-one algorithm has been adopted.  $C_{10}^2 = 45$  double classifiers are necessary for 10 types of postures.

### 3.2 ESF system

The ESF is intended to provide the amputees with the grasp force concept through stimulus grades

to transform hand grasp into cognitive dual grasp activities. The system consists of three electro-cutaneous electrodes corresponding to three hand motors, an electro-cutaneous stimulator (which drives the electro-cutaneous electrodes), and a top controller. We built a simple electro-cutaneous stimulator system to deliver sensory feedback to the user so as to provide him/her with extended perception. The power supply of stimulator circuit is provided from 7.2 V lithium batteries. The circuit system consists of power module A and electro-cutaneous stimulus module B (Fig. 4). The original 7.2 V enters into the fundamental chip (LM2577 by TI) of the power module, and after filtering and inductance, arrives at the 4th foot of the chip as the chip's switch voltage. Through compound commutation diode and electrolysis capacitance, the working voltage of the electro-cutaneous stimulator can be obtained as

$$V_{\text{out}} \text{ (V)} = 1.23 \left( \frac{R_{59}}{R_{63}} + 1 \right) \in [30, 33], \quad (6)$$

where 1.23 V is the output voltage of LM2577. For  $V_{\text{out}}$  in module A, the voltage pulse and surge current have been eliminated through ceramic capacitance

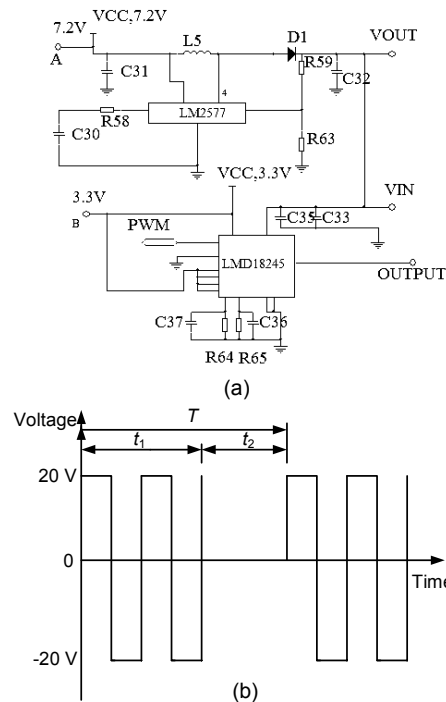


Fig. 4 Diagram (a) and output pulse (b) of electro-cutaneous sensory feedback (ESF)

C33 and aluminum electrolysis capacitance C35, respectively. Subsequently,  $V_{out}$  enters into the fundamental chip (LMD18245) of the electro-cutaneous stimulus as the driving voltage. The detective current from R64 works as the input for the inside current comparator. It is first compared with the inside DAC OUT, then deduces PWM signal through a uni-stable state, and finally realizes chopper control for the H-bridge output current. The RC net at the 3rd foot of the chip is used to adjust the switch interval of the H-bridge inside the fundamental chip:

$$T_{off \rightarrow on} = 1.1RC. \quad (7)$$

Continuous and biphasic square wave with 1 kHz frequency is applied as stimulus (Scott *et al.*, 1980), where  $t_1$  is the stimulation time,  $t_2$  is the intermission, and  $T$  is the stimulation cycle. Through different pulse width modulation (PWM) duty cycles, six skin stimulation grades corresponding to six grasp force grades are realized to provide the amputees with different grasp force perception (Table 1).

**Table 1 Relationship between the grade of electro-cutaneous stimulus, frequency, percentage of duty cycle, and exerting force**

Grade	Frequency (Hz)	Percentage of duty cycle	Force at fingertip (N·m)
1	2	0.46%	<0.05
2	10	2.3%	0.05–0.25
3	20	4.6%	0.25–0.45
4	40	9.2%	0.45–0.65
5	80	18.4%	0.65–0.85
6	120	27.6%	>0.85

The stimulus current, output voltage, and greatest stimulus frequency in the skin are 8 mA, ±20 V, and 120 Hz respectively, which are completely in the scope of clinical and experimental use for the subjects (Grill and Mortimer, 1996; Merrill *et al.*, 2005; Davidovics *et al.*, 2011) and may cause little irritation of the subjects. In the experiments the electro-cutaneous electrodes worked stably and delayed by only 50 ms, which cannot be felt by the user.

The ESF controller board is fixed in a top controller box. The actual grasp force information is sampled from base joint torques, transmitted to the top controller through the eCAN (controller area network) bus, reaches the ESF controller board

through the serial peripheral interface (SPI) bus, and produces the electro-cutaneous stimulus wave form. Therefore, the electro-cutaneous stimulator can bring forward grasp force feedback so that the subject can sense and control grasp forces during the EMG control grasp phase. Through provision of feeling information, the trained amputee can establish the relationship between electro-cutaneous current intensity and grasp power without relying on slide or thermo sensors. The ESF system helps transform hand grasp into cognitive dual grasp activities and plays a very important role in reducing the hand mis-manipulation and force bringing mistakes.

## 4 Experiments

### 4.1 EMG control

In the experiments, EMG signals were acquired from two healthy subjects. One (male) had been engaged in correlated muscular training for more than a year (testee M), and the other (female) had no experience at all (testee F). The following paragraph gives the EMG experimental protocols (Fig. 5).

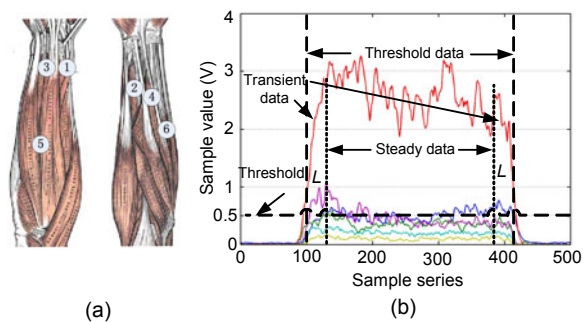


**Fig. 5 EMG experimental protocols**  
(a) Location of electrodes; (b) Training data states

Six Otto-Bock 13E200 electrodes were placed rationally on six groups of muscles (Table 2). For every experiment assembly there were four groups. The first two each consisted of four identical sessions, while the others each included three. The interval between each experiment assembly was at least two hours. Between each session, there was half an hour rest. In each session, experiments of all the 10 motion patterns above would be carried out five times. For every pattern, sampling would last 5 s with 100 Hz frequency. During sampling processes, the subject

was asked to relax→contract→hold on→relax the correlated muscles according to every pattern. The state of holding on must occupy over half of the data length. Such rapid contraction of specific muscles could easily lead to muscle fatigues, and thus could involve the EMG signals with some fatigue information.

**Table 2 Relationship between muscles and the prosthetic hand**

No.	Finger movement (basic pattern)	Muscle's scientific name
1	Thumb extension (1, 0, 0)	Extensor primi internodii pollicis
2	Thumb bending (-1, 0, 0)	Flexor pollicis longus muscle
3	Index finger extension (0, 1, 0)	Extensor indicis proprius (index finger)
4	Index finger bending (0, -1, 0)	Flexor digitorum superficialis muscle (index finger)
5	The other three fingers extension (0, 0, 1)	Extensor digitorum communis muscle and extensor digiti quinti proprius
6	The other three fingers bending (0, 0, -1)	Flexor digitorum superficialis muscle (three fingers)

The following is the training process according to Section 3.1.

1. Obtain the training sample data set  $\{(x_i, y_i) | i=1, 2, \dots, n\}$ , where  $y_i \in \{-1, 1\}$ .

In each session, 500 series of data (each series includes 10 samples) are obtained as Raw Data. If the data of all the channels is less than 0.5 V, the samples will be analyzed to obtain the Threshold Data. Transient Data is truncated at length  $L$  before and after the Threshold Data, respectively, to acquire Steady Data (Fig. 5).

(1) Threshold Data: There are  $C_9^2$  SVMs for the classification of nine motion patterns (inspiring states) during training with Threshold Data, since at the relaxation state (pattern (0, 0, 0)) there is no Threshold Data.

(2) Steady Data: Taking the place of the relaxation state with the first four groups of Raw Data,  $C_{10}^2$  SVMs are needed to solve all the 10 motion patterns.

Proof: The data series of the fifth group of Raw Data is applied to prove SVMs with:

(3) Threshold Data: All inspiring states are in series to simulate the real-time state motion patterns.

(4) Transient Data: This is the process from the muscle start up movement until the movement becomes stable. The length is 25 transient points.

2. Construct and solve the optimized problem according to Eq. (5) to obtain the optimal solution  $\beta^* = (\beta_1^*, \beta_2^*, \dots, \beta_n^*)^T$ .

3. Compute  $b^* = y_j - \sum_{i=1}^n \beta_i^* y_i K(x_i, x_j)$  and  $\sum_{i=1}^n \beta_i^* y_i x_i$ .

4. Solve the decision function (5) according to the hyperplane (Eq. (1)).

The set of  $C=2^6$  and  $\gamma=2^{-3}$  is the most effective and typical, according to massive search experiments on the choice of  $C$  and  $\gamma$  (which are both at the base of 2) at the ranges of  $[2^2, 2^8]$  and  $[2^{-4}, 2^2]$ , respectively. In Fig. 6, characters I and II denote training while character III denotes success ratio proof. For example, M(I,III) represents the success ratios when testee M was trained by clustering I and proved with clustering III, while M(I) represents the ratio from testee M trained by clustering I. Others are similar. Although testees could achieve higher training success ratios with clustering II (Fig. 6a), clustering II obtained lower proof ratios than clustering I. In comparison with testee M, testee F obtained lower but improving success ratios. For the 10 motion patterns listed above, the proof success ratios of testee M were larger than 95% and very stable. Testee F achieved the same high ratios in the 4th and 5th sessions. In other words, trained persons can achieve almost the same high successful classification and identification ratios.

For training with pattern groups (Fig. 6b), pattern I can improve the identification capacity by almost 20%. At the beginning, identification errors occurred frequently for IV, but the success ratio would increase with experience.

After SVM classifiers have been established, the 10 motion patterns in Fig. 7 can be recognized in real time. The controller can not only command the motors to make corresponding movements, but also attain the follow-up effects before the human hand postures became stable. Therefore, continuous motion control can be performed, if commands are continuously sent to the hand controller at a certain frequency.

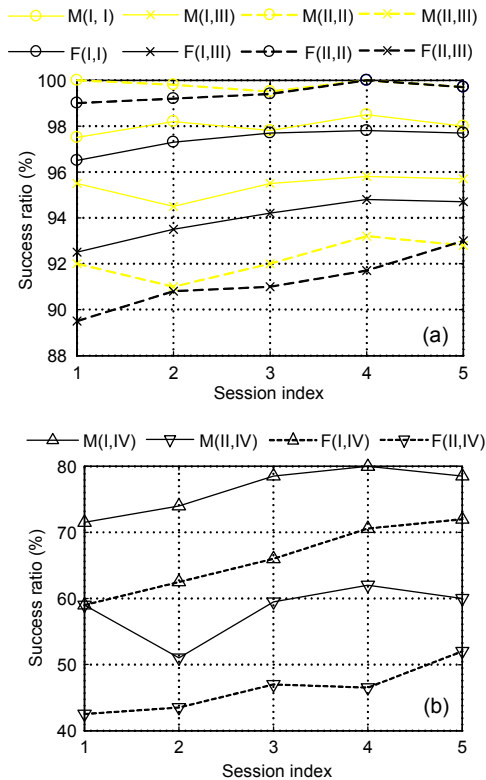


Fig. 6 The success ratios of training and proving ( $C=2^6$  and  $\gamma=2^{-3}$ ) during the entire five sessions (a) and transitional data clustering (IV) identification (b)

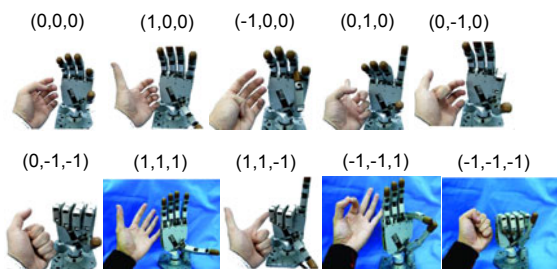


Fig. 7 The 10 motion patterns in experiments

#### 4.2 Cognitive experiments with the ESF system

To eliminate the interference with the EMG, the ESF electrodes were placed on the upper limb (Fig. 8a and Table 3: points A, B, and C corresponding to the thumb, index finger, and the other three fingers, respectively). There is a dead time (when there is no signal) in the recordings following the EMG current to further filter out bad EMG signals, and similarly for the stimulation feedback current. Correlation of ESF signals at every frequency was detected and compared to ascertain the most desirable positions.

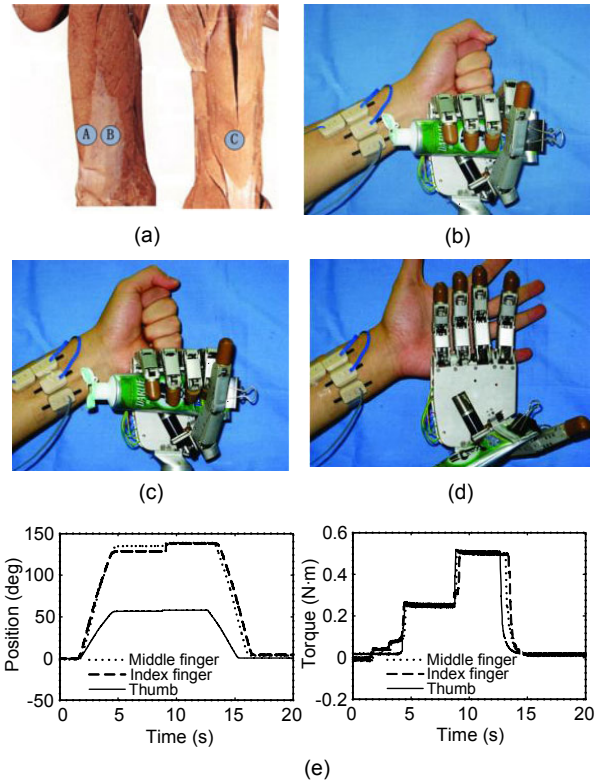


Fig. 8 Toothpaste crushing experiment

(a) Location of vibration motors; (b) 4.6% PWM duty cycle; (c) 9.2% PWM duty cycle; (d) 0 PWM duty cycle (hand relax); (e) Position and force response of the fingers' base joints during crushing; (f) Crushing force selection scheme (the user could select the force through the algorithm proposed by Huang et al. (2010))

Table 3 Upper limb muscles and ESF stimulus

No.	ESF electrode	Corresponding finger's grasp force	Muscle's scientific name
1	A	Thumb	Triceps brachii long head
2	B	Index finger	Triceps brachii lateral head
3	C	The other three fingers	Biceps brachii long head

Provided with electro-cutaneous stimulation, the user–prosthesis interface has been established. User’s concentration and interaction are more involved to decide how to perform and when to stop the grasp.

In a toothpaste crushing experiment (Fig. 8), traditional prostheses executed the crushing action as follows. In the first phase, the hand was driven in its preshaping posture. Secondly, the hand closes the corresponding fingers according to the preset force. Grasp force can be controlled only through visual feedback. The users’ capability to decide how to perform the crush is very low, because limited concentration and interaction are involved. When ESF is involved, the hand is first pre-shaped through EMG command. Then, a flexor contraction attempt ensures that they commence the closure state. Through a cognitive dual process from visual feedback and ESF, the subject getting to know the grasp force may be comparatively small at first. The subject could achieve a stronger prehension state crush. In other words, he/she could sense and select the grasp force through the ESF system or the force control algorithm proposed by Huang *et al.* (2010) to decide how much toothpaste to crush out. The ESF system helped the subject understand the force and crush skillfully. Hence, by paying attention to ESF, users are able to decide how much closure force should be applied for crushing.

The 3rd subject had been engaged in both correlated EMG muscular training for a few months and ESF research & experiments for half a year. He performed some other experiments (Table 4) about the cognitive dual grasp process under the following protocols: During the grasp experiments without ESF (NESF), the subject identified objects first by vision

to decide the grasp pattern and anticipate force requirements. Then he looked at the prosthesis during its operation, but he was not sure how to perform the desirable grasp. Grasps were considered successful when the objects had been correctly lifted off (i.e., no slippage event occurs; otherwise, the object has to try again). During the grasp experiments with ESF (WESF), however, the grasp process is a cognitive dual grasp activity to select both hand preshape and force closure. Visual feedback and ESF are essential in deciding how to perform and when to stop increasing the grasp force. The overall experiments (Table 4) lasted 20 days. The subject grasped all the objects 10 times in an hour no matter whether the grasp was successful or not. The subject grasped each object 1000 times, NESF 500 times and WESF 500 times. All the NESF experiments proceeded first.

Take ‘pinch’ grasp (P1) as an example. First ‘pinch’ grasp was chosen through EMG commands. Then the subject estimated the desired finger force through the following equation, after the fingers have been positioned:

$$F_p = \begin{cases} F_C / 2, & p = 1, \\ 0, & p = 3, \\ F_C / 2, & p = 2, \end{cases} \quad (8)$$

where  $F_C$  is the force closure of the ‘pinch’ and  $p$  is an index referring to fingers: 1 denotes the thumb, 2 denotes the index finger, and 3 denotes the other three fingers. Subsequently, the subject started pinching by means of flexor contraction. Through the cognitive dual process from visual feedback and ESF, the subject knew whether the grasp force is adequate or not and decided how to perform the pinch.

**Table 4 Different objects for grasp**

Grasp type	Object	ID	Size $D$ (cm)	Weight (g)	Grade of electro-cutaneous stimulus
Grasp	Small bottle	G1	5.0	200	4
	Big bottle	G2	8.5	800	6
	Small cylinder	G3	4.5	100	3
	Big cylinder	G4	8.0	200	5
	Heavy and big cylinder	G5	8.5	750	6
	Complex shape	G6		100	4
	Heavy object with complex shape	G7		830	6
Hook	Pen	H1	1.8	60	2
	Steel stick	H2	2.0	200	5
Pinch	Coin	P1	4.0	80	2

For comparison, three vibrotactile motors were used as sensory feedback corresponding to three electro-cutaneous electrodes under the same experimental protocols and conditions. Fig. 9 implies that the prosthetic hand was more successful in power grasp, light circular ‘hook’ and ‘pinch’ with sensory feedback. For cognitive dual grasp activities of a healthy subject, ESF worked better in light circular ‘hook’ and ‘pinch’ because skin is more sensitive to stimulation, whereas vibrotactile feedback worked better in power grasp because higher vibration frequency is easier to distinguish.

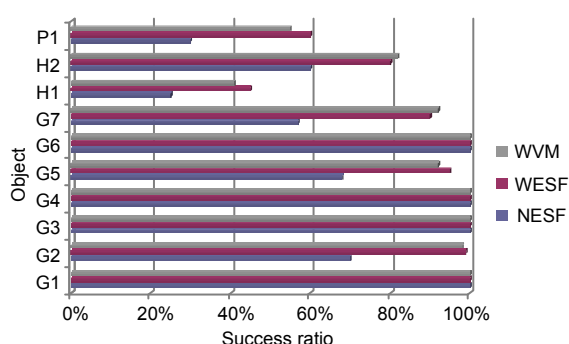


**Fig. 9** Grasp experiment results (see Table 4 for details of the objects)

WESF: with ESF; NESF: without ESF; WVM: with vibrotactile motor

### 4.3 Voice control

Voice control is an assistant method for EMG recognition through voice signal recognition. The voice signals were acquired and processed by a special voice chip on the voice signal disposal board. A special voice chip accomplishes voice recognition through feature extraction of voice, resemblance calculation, and judgments. The conversion results were transmitted to a DSP system through the Bluetooth wireless protocol and transformed into the control instruction for hand operation.

Table 5 illustrates three voice commands to control the hand (Fig. 10). The voice could successfully control the hand through Bluetooth wireless transmission in a quiet environment.

**Table 5** Instructions of voice recognition

No.	Voice (motion) pattern	Instruction
1	Grasp	F700AA11AA11
2	Unclench	F700AD41AD41
3	Pinch	F700AC31AC31

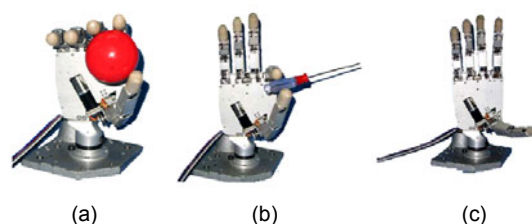


**Fig. 10** Pattern recognition for voice control  
(a) Grasp; (b) Pinch; (c) Release (Unclench)

Different from EMG recognition, the results of voice control are decided by complicated factors. They are not only affected by characteristics of human speech such as loudness, frequency, accent, tone, and pitch, but also greatly influenced by various environmental noises. Currently voice control of HIT/DLR Prosthetic Hand II can work well only in a quiet environment as a kind of assistant method. For application in different daily noisy environments, great efforts have to be made in the areas of recognition algorithms, training measurement, and so on.

### 4.4 Experiments with an amputee

Further experiments were performed with a 45 years old male amputee from the Prosthesis Center of Heilongjiang Province, China. He had been amputated for five years and nearly 3/5 of his right forearm was amputated. Musculature of the forearm remained so incomplete that the locations of electrodes were affected. Though having been a customer of Otto Bock Sensor Hand for years, EMG signals of many patterns were still crossing and uncertain. It is difficult to find corresponding forearm muscle positions, because the damages and suture of the nerve and muscle tissue of this amputee were unclear. To ascertain the most desirable EMG electrode positions, primary positions were adjusted in consideration of the subject’s feelings and signal amplitude (Fig. 11). EMG control had to be realized by remapping muscle contraction with prosthetic hand movement.

With the same experimental protocols as in Section 4.1, the amputee made the same 10 pattern recognition experiments as testees M and F. The success ratios of the 5th session are issued in Table 6. For the amputee, the high success ratios of patterns 7, 15, 19, and 24 indicate effective recognition in extension of the thumb, and bending and extension of the other three fingers. The high success ratios of patterns 26 and 27 in Table 6 were obtained through cluster

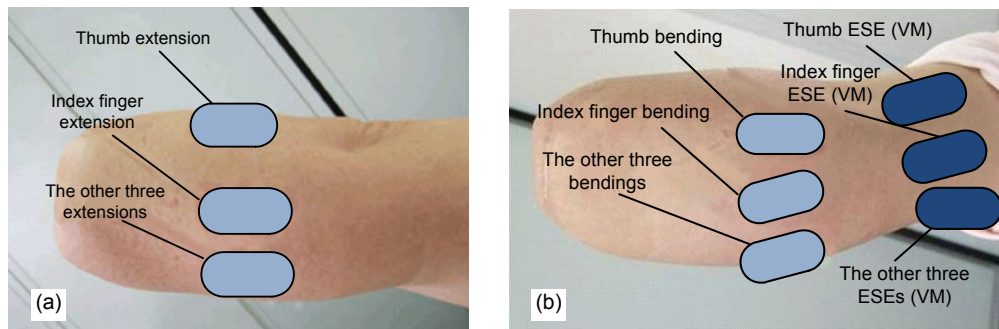


Fig. 11 Positions of EMG (a) and electro-cutaneous stimulus electrodes (ESEs) (b)

Table 6 Hand pattern recognition success ratios of the amputee

Pattern	Success ratio (%)									
	1	2	7	9	10	15	19	24	26	27
(I)		73.85	98.85	94.81	82.34	96.38	97.51	94.58	96.76	93.71
(II)	94.7	74.75	99.25	95.05	82.85	97.05	97.55	95.03	97.27	93.88
(I,III)		69.07	91.29	93.71	74.75	93.02	94.23	94.08	95.21	92.14
(II,III)		68.09	99.35	92.70	73.85	92.65	94.81	94.49	94.72	90.01

analysis (based on the Euclidean distance) and overlapping samples elimination. The success ratios of pattern 9 were similar to those of pattern 26, because all the fingers except the thumb were bending in this pattern. Since it is easier for the amputee to realize the finger movement of all bending-extension than all bending-relaxation-extension, the success ratios of patterns 26 and 27 were 73% and 74%, respectively at the beginning. Success ratios of patterns 2 and 10 were low because there was much crossing information in thumb bending and index finger extension. Therefore, the amputee can provide signals of eight grasp patterns (1, 7, 9, 15, 19, 24, 26, and 27) very successfully after training.

With the same experimental protocols as in Section 4.2, the amputee did the same experiments as the third subject in Table 4. The electro-cutaneous stimulus electrodes or vibrotactile motors (VM) were placed on the upper limb. Correlation of electro-cutaneous stimulus electrodes (or VM) at every frequency was detected and compared to ascertain the most desirable positions. After days of training, the experiments began.

Fig. 12 implies that the cognitive dual grasp process of vision and force feedback is more successful in power grasp, light circular 'hook' and 'pinch' for the amputee. For the amputee with damages and suture of his nerve, skin stimulation may work better than vibration feelings.

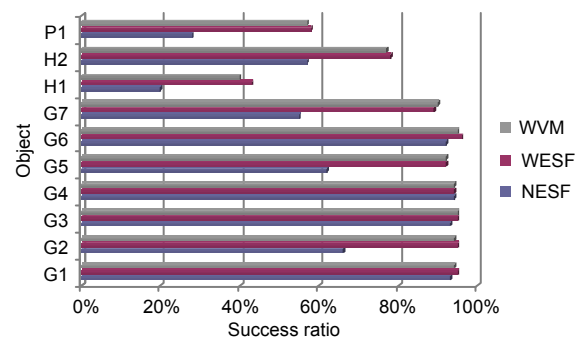


Fig. 12 Grasp experimental results of the amputee (see Table 4 for details of the objects)

WESF: with ESF; NESF: without ESF; WVM: with vibrotactile motor

## 5 Conclusions

This paper brings forward an anthropomorphic controller for EMG multi-posture recognition and cognitive dual grasp activities of the prosthetics hand system.

An optimal separating hyperplane was found through the RBF kernel for SVM pattern classification and recognition. Ten types of hand postures were successfully recognized by six electrodes. The hierarchical shared control between the top controller and the prosthesis-embedded low-level controller has provided the subject-prosthesis interface for cogni-

tive dual grasp activities.

Experiments on EMG multi-pattern recognition and ESF were carried out on three subjects and an amputee. The success ratios for multi-pattern recognition are very high. The ESF cognitive dual grasp process shows the advantage related to sensory feedback. This process increases users' concentration and interaction during the grasp phase, and improves the hand power grasp, light circular 'hook' and 'pinch' success ratios. Experiments with the amputee have further verified the effectiveness of the hierarchical control strategies and indicated its application potentials.

## References

- Ajiboye, A.B., Weir, R.F.F., 2005. A heuristic fuzzy logic approach to EMG pattern recognition for multifunctional prosthetic control. *IEEE Trans. Neur. Syst. Rehabil. Eng.*, **13**(3):280-291. [doi:10.1109/TNSRE.2005.847357]
- Antfolk, C., Balkenius, C., Lundborg, G., Rosén, B., Sebelius, F., 2010. Design and technical construction of a tactile display for sensory feedback in a hand prosthesis system. *BioMed. Eng. OnLine*, **9**:50. [doi:10.1186/1475-925X-9-50]
- Bicchi, A., 2000. Hand for dexterous manipulation and robust grasping: a difficult road toward simplicity. *IEEE Trans. Robot. Autom.*, **16**(6):652-662. [doi:10.1109/70.897777]
- Bitzer, S., van der Smagt, P., 2006. Learning EMG Control of a Robotic Hand: Towards Active Prostheses. IEEE Int. Conf. on Robotics and Automation, p.2819-2823. [doi:10.1109/ROBOT.2006.1642128]
- Burges, C.J.C., 1998. A tutorial on support vector machines for pattern recognition. *Data Min. Knowl. Disc.*, **2**(2):121-167. [doi:10.1023/A:1009715923555]
- Castellini, C., van der Smagt, P., 2009. Surface EMG in advanced hand prosthetics. *Biol. Cybern.*, **100**(1):35-47. [doi:10.1007/s00422-008-0278-1]
- Clement, R.G.E., Bugler, K.E., Oliver, C.W., 2011. Bionic prosthetic hands: a review of present technology and future aspirations. *Surgeon*, **9**(6):336-340. [doi:10.1016/j.surge.2011.06.001]
- Dario, P., Laschi, C., Carrozza, M.C., Guglielmelli, E., Teti, G., Massa, B., Zecca, M., Taddeucci, D., Leoni, F., 2002. An Integrated Approach for the Design and Development of a Grasping and Manipulation System in Humanoid Robotics. IEEE Int. Conf. on Robotics & Automation, **1**:1-7.
- Davidovics, N.S., Fridman, G.Y., Chiang, B., Della Santina, C.C., 2011. Effects of biphasic current pulse frequency, amplitude, duration, and interphase gap on eye movement responses to prosthetic electrical stimulation of the vestibular nerve. *IEEE Trans. Neur. Syst. Rehabil. Eng.*, **19**(1):84-94. [doi:10.1109/TNSRE.2010.2065241]
- Dechev, N., Cleghorn, W.L., Naumann, S., 2001. Multiple finger, passive adaptive grasp prosthetic hand. *Mech. Mach. Theory*, **36**(10):1157-1173. [doi:10.1016/S0094-114X(01)00035-0]
- Della Santina, C.C., Migliaccio, A.A., Patel, A.H., 2007. A multichannel semicircular canal neural prosthesis using electrical stimulation to restore 3-D vestibular sensation. *IEEE Trans. Biomed. Eng.*, **54**(6):1016-1030. [doi:10.1109/TBME.2007.894629]
- Diftler, M.A., Culbert, C.J., Ambrose, R.O., Platt, R.Jr., Bluethmann, W.J., 2003. Evolution of the NASA/DARPA Robonaut Control System. IEEE Int. Conf. on Robotics and Automation, **2**:2543-2548. [doi:10.1109/ROBOT.2003.1241975]
- Edsinger-Gonzales, A., 2004. Design of a Compliant and Force Sensing Hand for a Humanoid Robot. Proc. Int. Conf. on Intelligent Manipulation and Grasping, p.291-295.
- Graupe, D., Salahi, J., Kohn, K., 1982. Multifunction prosthesis and orthosis control via micro-computer identification of temporal pattern differences in single-site myoelectric signals. *J. Biomed. Eng.*, **4**(1):17-22. [doi:10.1016/0141-5425(82)90021-8]
- Grill, W.M.Jr., Mortimer, J.T., 1996. The effect of stimulus pulse duration on selectivity of neural stimulation. *IEEE Trans. Biomed. Eng.*, **43**(2):161-166. [doi:10.1109/10.481985]
- Huang, H., Jiang, L., Zhao, D.W., Zhao, J.D., Cai, H.G., Liu, H., Meusel, P., Willberg, B., Hirzinger, G., 2006. The Development on a New Biomechatronic Prosthetic Hand Based on Under-Actuated Mechanism. IEEE/RSJ Int. Conf. on Intelligent Robots and Systems, p.3791-3796. [doi:10.1109/IROS.2006.281765]
- Huang, H., Jiang, L., Pang, Y.J., Shi, S.C., Tang, Q.R., Yang, D.P., Liu, H., 2010. Observer-based dynamic control of an underactuated hand. *Adv. Robot.*, **24**(1-2):123-137. [doi:10.1163/016918609X12586151361812]
- Huang, H.P., Chen, C.Y., 1999. Development of a Myoelectric Discrimination System for a Multi-degree Prosthetic Hand. Proc. IEEE Int. Conf. on Robotics and Automation, p.2392-2397.
- Jacobsen, S.C., Iversen, E.K., Knutti, D.F., Johnson, R.T., Biggers, K.B., 2001. Design of the Utah/MIT Dextrous Hand. IEEE Int. Conf. on Robotics and Automation, p.1520-1532.
- Kawasaki, H., Mouri, T., Ito, S., 2004. Toward Next Stage of Kinetic Humanoid Hand. 10th Int. Symp. on Robotics with Applications, p.129-134.
- Keerthi, S.S., Lin, C.J., 2003. Asymptotic behaviors of support vector machines with Gaussian kernel. *Neur. Comput.*, **15**(7):1667-1689. [doi:10.1162/089976603321891855]
- Kuiken, T., Marasco, P., Lock, B., Harden, R., Dewald, J., 2007. Redirection of cutaneous sensation from the hand to the chest skin of human amputees with targeted reinnervation. *PNAS*, **104**(50):20061-20066. [doi:10.1073/pnas.0706525104]
- Kumar, P., Sebastian, A., Potluri, C., Urfer, A., Naidu, D.S., Schoen, M.P., 2010. Towards Smart Prosthetic Hand: Adaptive Probability Based Skeletan Muscle Fatigue

- Model. 32nd Annual Int. Conf. IEEE EMBS, p.1316-1319. [doi:10.1109/IEMBS.2010.5626388]
- Lee, H.C., Kang, B.J., Lee, E.C., Park, K.R., 2010. Finger vein recognition using weighted local binary pattern code based on a support vector machine. *J. Zhejiang Univ.-Sci. C (Comput. & Electron.)*, **11**(7):514-524. [doi:10.1631/jzus.C0910550]
- Lee, S., Saridis, G.N., 1984. The control of a prosthetic arm by EMG pattern recognition. *IEEE Trans. Autom. Control*, **29**(4):290-320. [doi:10.1109/TAC.1984.1103521]
- Liu, H., Meusel, P., Seitz, N., Willberg, B., Hirzinger, G., Jin, M.H., Liu, Y.W., Wei, R., Xie, Z.W., 2007. The modular multisensory DLR-HIT-Hand. *Mech. Mach. Theory*, **42**(5): 612-625. [doi:10.1016/j.mechmachtheory.2006.04.013]
- Liu, Y.H., Huang, H.P., Weng, C.H., 2007. Recognition of electromyographic signals using cascaded kernel learning machine. *IEEE/ASME Trans. Mechatron.*, **12**(3):253-264. [doi:10.1109/TMECH.2007.897253]
- Lotti, F., Tiezzi, P., Vassura, G., Biagiotti, L., Palli, G., Melchiorri, C., 2005. Development of UB Hand 3: Early Results. Proc. IEEE Int. Conf. on Robotics and Automation, p.4488-4493. [doi:10.1109/ROBOT.2005.1570811]
- Loucks, C.S., Johnson, V.J., Boissiere, P.T., Starr, G.P., Steele, J.P.H., 1987. Modeling and Control of the Stanford/JPL Hand. Int. Conf. on Robotics and Automation, p.573-578.
- Merrill, D.R., Bikson, M., Jefferys, J.G., 2005. Electrical stimulation of excitable tissue: design of efficacious and safe protocols. *J. Neurosci. Methods*, **141**(2):171-198. [doi:10.1016/j.jneumeth.2004.10.020]
- Micera, S., Carpaneto, J., Raspopovic, S., 2010. Control of hand prostheses using peripheral information. *IEEE Rev. Biomed. Eng.*, **3**:48-68. [doi:10.1109/RBME.2010.2085429]
- Pylatiuk, C., Mounier, S., Kargov, A., Schulz, S., Bretthauer, G., 2004. Progress in the Development of a Multifunctional Hand Prosthesis. Proc. 26th Annual Int. Conf. IEEE EMBS, p.4260-4263.
- Rosen, B., Ehrsson, H., Antfolk, C., Cipriani, C., Sebelius, F., Lundborg, G., 2009. Referral of sensation to an advanced humanoid robotic hand prosthesis. *J. Plast. Reconstr. Surg. Hand Surg.*, **43**(5):260-266. [doi:10.3109/02844310903113107]
- Scott, R.N., Caldwell, R.R., Britain, R.H., 1980. Sensory-feedback system compatible with myoelectric control. *Med. Biol. Eng. Comput.*, **18**(1):65-69. [doi:10.1007/BF02442481]
- Shimizu, S., Shimojo, M., Sato, S., Seki, Y., Takahashi, A., Inukai, Y., Yoshioka, M., 1997. The Relationship Between Human Grip Types and Force Distribution Pattern in Grasping. Proc. 8th Int. Conf. on Advanced Robotics, p.299-304.
- Stepp, C.E., Matsuoka, Y., 2011. Object manipulation improvements due to single session training outweigh the differences among stimulation sites during vibrotactile feedback. *IEEE Trans. Neur. Syst. Rehabil. Eng.*, **19**(6): 677-685. [doi:10.1109/TNSRE.2011.2168981]
- Taylor, C.L., Schwarz, R.J., 1955. The anatomy and mechanics of the human hand. *Artif. Limbs*, **2**:22-35.
- Wimböck, T., Ott, C., Hirzinger, G., 2007. Impedance Behaviors for Two-Handed Manipulation: Design and Experiments. IEEE Int. Conf. on Robotics and Automation, p.4182-4189. [doi:10.1109/ROBOT.2007.364122]
- Zhao, J.D., Xie, Z.W., Jiang, L., Cai, H.G., Liu, H., Hirzinger, G., 2005. Levenberg-Marquardt Based Neural Network Control for a Five-Fingered Prosthetic Hand. Proc. IEEE Int. Conf. on Robotics and Automation, p.4482-4487. [doi:10.1109/ROBOT.2005.1570810]
- Zhao, J.D., Xie, W.X., Jiang, L., Cai, H.G., Liu, H., Hirzinger, G., 2006. A Five-Fingered Underactuated Prosthetic Hand Control Scheme. First IEEE/RAS-EMBS Int. Conf. on Biomedical Robotics and Biomechanics, p.995-1000. [doi:10.1109/BIOROB.2006.1639221]
- Zollo, L., Roccella, S., Tucci, R., Siciliano, B., Guglielmelli, E., Carrozza, M.C., Dario, P., 2006. BioMechatronic Design and Control of an Anthropomorphic Artificial Hand for Prosthetics and Robotic Applications. First Int. Conf. on Biomedical Robotics and Biomechanics, p.402-407. [doi:10.1109/BIOROB.2006.1639121]
- Zollo, L., Roccella, S., Tucci, R., Siciliano, B., Guglielmelli, E., Carrozza, M.C., Dario, P., 2007. Biomechatronic design and control of an anthropomorphic artificial hand for prosthetic and robotic applications. *IEEE/ASME Trans. Mechatron.*, **12**(4):418-429. [doi:10.1109/TMECH.2007.901936]